RAPID ASSESSMENT OF AS-GROWN INTERSTITIAL IRON CONCENTRATION AND IMPACT ON P-TYPE SILICON BLOCKS VIA SPECTRAL PHOTOLUMINESCENCE IMAGING

Bernhard Mitchell[1], Daniel Macdonald[2], Jonas Schön[3], Jürgen W. Weber[4], and Thorsten Trupke[1,4]

[1] Australian Centre for Advanced Photovoltaics, University of New South Wales, Sydney, Australia
[2] Research School of Engineering, The Australian National University, Canberra, Australia
[3] Fraunhofer Institute for Solar Energy Systems, Freiburg, Germany
[4] BT Imaging Pty Ltd, Sydney, Australia

ABSTRACT: Early stage material quality control directly after crystallization is becoming increasingly sophisticated. It is enabled through the characterization of various material parameters along the silicon ingot/brick side faces. Photoluminescence techniques can provide quantitative measures for example of the important photovoltaic material parameter of bulk lifetime. It can measure this parameter with full spatial resolution within a few seconds. Here, we demonstrate the extension of the spectral photoluminescence analysis on silicon bricks to the extraction of the dissolved iron concentration. The analysis uses 1) the reversible pairing that interstitial iron undergoes with the acceptor atom at room temperature in the dark after iron boron pairs were dissociated with an intense flashlight and 2) the respective lifetime fingerprint of these fairly well known defects. We can perform the analysis without any extra sample preparation on the bare brick, measure at true low injection conditions and are able to integrate it into a production environment. We demonstrate the analysis on a widely used 6 inch multicrystalline silicon brick that was directionally solidified from electronic grade feedstock. With access to both bulk lifetime and interstitial iron concentration, the relative impact of the interstitial iron concentration can be quantified and a theoretical bulk lifetime after removal of all interstitial iron contamination can be calculated. Both of these represent interesting early and direct measures relevant to the further understanding of the crystallization and following cell processing. Interstitial iron has been found to contribute majorly to the overall recombination all through the as-grown ingot and is dominating the recombination in the highly contaminated and low lifetime bottom of the ingot. The combined access to spatial information of both bulk lifetime and interstitial iron concentration is found to be a valuable tool to also assess the contribution of other defect contaminations, its distributions and, with some additional information aside, possibly also its origins and causes.

Keywords: Interstitial iron, Dissolved iron, Photoluminescence Imaging, Silicon, Ingot, Bricks

1 INGOT CHARACTERISATION

Photoluminescence (PL) techniques for the characterization of silicon ingots have been systematically investigated in the recent years [1–3]. The extended bulk and the bare, but polished, surface of the squared brick provide a unique sample with defined properties that allow accurate modelling of the photoluminescence response during excitation with light.

The spontaneous radiative emission caused by the band-to-band recombination in silicon is a weak signal, but has been shown sufficiently intense for PL measurements on silicon bricks with a lifetime in the micro- to millisecond range. The PL spectrum emitted by the sample carries a certain bulk lifetime signature that is defined by a certain level of luminescence reabsorption on its optical path within the sample. A simple spectral ratio analysis can independently quantify the bulk lifetime and without the knowledge of the background doping.

The spectral PL analysis can be done pixel by pixel in an imaging application with sufficient signal to noise ratio (SNR). Thus, it allows the assessment of material parameters within 10-20 seconds with megapixel resolution.

The minority carrier bulk lifetime is defined mostly via defect recombination in silicon. A prominent point defect is introduced by the transition metal iron. Dissolved iron occupies, particularly in its interstitial state, near mid-gap defect levels [4], which easily reduce the minority carrier lifetime. Concentrations as low as $1x10^{11}$ cm^{-3} [5] start reducing the bulk lifetime and thus the cell efficiency in p-type silicon.

The interstitial iron concentration has been measured on passivated silicon wafers using PL imaging techniques [6], and has since led to many interesting studies of the emergence of iron contamination throughout the cell processing. These were particularly interesting due to the high spatial resolution, sensitivity and reproducibility that PL imaging based analyses allowed for [7,8].

Here, we will demonstrate the use of PL imaging to extract information already on the bare surfaces of polished but otherwise unprepared silicon bricks vertical side faces. We thus gain access to the unaltered as-grown dissolved iron concentration. We will elaborate on the main aspects of the method, its results and discuss the validity of the data. A more detailed description of this new method has already been published elsewhere [9].

2 DISSOLVED IRON MEASUREMENT

It has been long known that interstitial iron Fe_i is positively charged in p-type Si at room- and slightly elevated temperatures. Thus, it readily forms a Coulomb pair with negatively charged defects such as shallow acceptors (boron, gallium, aluminum). However, excess carriers (e.g. injected by light) and elevated temperatures shift the equilibrium state to Fe_i being dissociated from its substitutional acceptor (e.g. boron). Under typical operation most dissolved iron is dissociated from the acceptor atom and occupies an interstitial lattice position.

Iron boron (Fe-B) pairs and the interstitial iron have different defect levels, thus causing a different injection-level dependent lifetime behavior. The latter can be modelled using the respective defect parameters and the Shockley-Read-Hall (SRH) formalism (see Figure 1).

The dissolved iron in the silicon ingot/brick can be intentionally cycled between the paired and the

dissociated interstitial state most easily by using an intense light source. The SRH calculations displayed in Figure 1 show that the respective lifetimes are not injection dependent below an injection level of about $1x10^{12}$ cm^{-3}, thus representing an ideal measurement regime limiting the experimental uncertainty resulting from the estimation of the injection level. Spectral PL intensity ratio imaging is able to assess the bulk lifetime at such low injection levels with sufficient SNR. Such injection level is achieved by reducing the illumination intensity to about 0.1 suns (0.01 W/cm^2) during measurement.

Samples with exceptionally high bulk lifetimes such as Cz-grown n-type ingots can be measured at even lower illumination intensity, thus retaining the injection independent measurement regime.

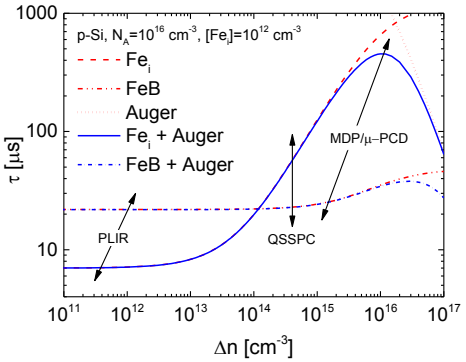

Figure 1: Calculated carrier lifetimes due to Fe_i and Fe-B pairs in boron-doped silicon with $N_A=10^{16}$ cm^{-3} and an iron concentration of 10^{12} cm^{-3} as a function of the excess carrier density Δn. Auger recombination and its impact on the lifetimes at high injection is also shown. The typical injection regions in which PLIR, QSSPC and MDP/µ-PCD operate are indicated.

In our experiments, we used a strong flash lamp that can provide short light pulses in excess of 1000 suns illumination intensity. Our modelling shows that this is sufficient to assume full dissociation of all Fe-B pairs [9]. A complete dissociation is crucial to allow for an accurate analysis as the fraction of a partial dissociation is difficult to assess.

The optimal measurement procedure would apply the light dissociation and measure the respective bulk lifetime, prior to measuring the paired lifetime, since boron oxygen related impacts on the bulk lifetime cannot be fully excluded in the bottom of the ingot and should not be mixed. However, this would increase the measurement time substantially, or effectively raise the need for two time-separate measurements.

In many practical cases, we believe the impact of boron oxygen can be neglected or generalized, thus allowing for a measurement cycle in the order of a few minutes by measuring the paired prior to the dissociated state.

Once the bulk lifetimes have been assessed using the spectral PL intensity ratio analysis, the iron concentration can be determined using the SRH recombination model as formulated by Zoth and Bergholz [10]:

$$[Fe_i] = C(\Delta n, N)\left\{\frac{1}{\tau_{b,f}} - \frac{1}{\tau_{b,i}}\right\}$$

where $\tau_{b,i}$ and $\tau_{b,f}$ are the initial and the final bulk lifetime, i.e. before and after Fe-B pair breaking.

3 RESULTS

We measured the dissociated bulk lifetime images on a standard-growth mc-Si brick using spectral PL intensity ratio analyses (reported in [1,2,11]) after applying sufficiently intense flash illumination to completely dissociate the Fe-B within the measured bulk region (see [2]). The resulting bulk lifetimes are shown in Figure 2 (left) and reveal lifetimes of up to about 60 µs centrally. The association time constant is dependent on the acceptor (boron) concentration [12]. A typical p-type ingot is fully repaired within a few hours in the dark.

The bulk lifetime of our sample ingot increased by 40-80% after complete repairing as illustrated in Figure 2 (right).

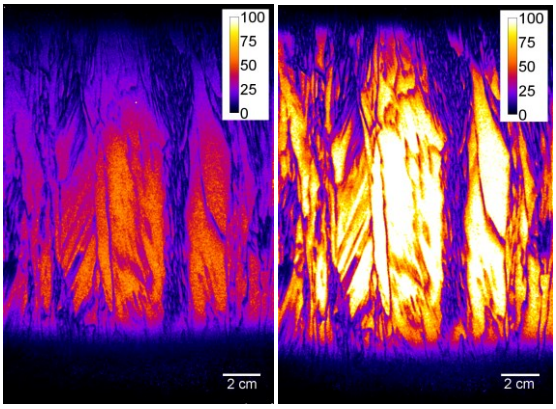

Figure 2: Spectral PLIR detected bulk lifetime images of standard-growth silicon brick after complete Fe-B pair dissociation (left) and fully repaired (right). As-grown bulk lifetimes are given in µs at weighted average injection levels ranging from $1x10^{11}$-$1x10^{12}$cm^{-3}.

We calculate the respective C-factor for our injection regime and doping concentration. The analysis is strongly simplified at injection levels below $1x10^{12}$ cm^{-3} , since the C-factor is neither injection nor significantly doping dependent in this regime (see Figure 1) [13]. Therefore, there is no need to calculate it pixel by pixel. Additionally, we also can be more confident not to introduce an additional uncertainty due to the injection dependence [9].

The resulting dissolved iron concentration image is depicted in Figure 3 on logarithmic scale. We find a contamination level of $0.9x10^{11}$ cm^{-3} in the lower central region that increases slowly towards up to $1x10^{12}$ cm^{-3} near the top indicating the iron segregation during crystal growth.

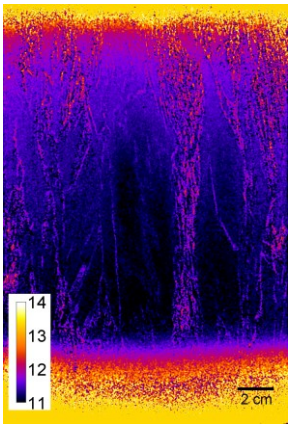

Figure 3: Log_{10} [Fe_i] images of standard-growth mc-Si bricks. As-grown dissolved iron concentrations are given in cm^{-3}. The data in the highly contaminated bottom and top sections of the bricks is not quantitative when derived from a simple full-field analysis, but can be assessed quantitatively using a masking approach (see [9]).

The bottom and top regions of the ingot that are affected by in-diffusion from the crucible and lining could not be assessed directly, due to limiting light spreading in the SiCCD detector [2], which currently represents the main limitation of the spectral analysis in full-field PL measurements on silicon ingots. However, alternative approaches that include a masking of the central high lifetime area during the measurement have been able include the low lifetime bottom and top region into the measurement and found contamination levels in the range of 1-4x10^{13} cm^{-3} [9].

With access to both bulk lifetime and interstitial iron concentration, it is possible to rate the relative impact of the interstitial iron induce recombination using the SRH lifetimes. Figure 4 presents the results for the sample ingot discussed in this work. It reveals major to dominant recombination through the interstitial iron defect level. Both bottom and top regions are nearly completely dominated by recombination through interstitial iron. The lowest values are around found at about 30% height where approximately 60% of the total recombination is through interstitial iron defect levels after crystal growth. Note that this recombination fraction is vastly altered by following gettering and hydrogenation steps. Here, the remaining impact of iron contamination depends individually on many parameters which are largely influenced by the respective cell design and its processing requirements.

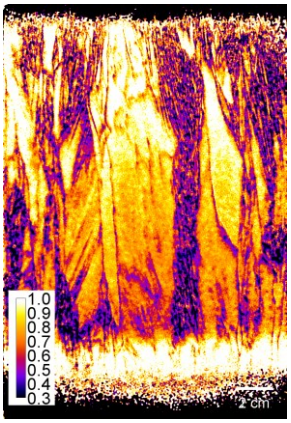

Figure 4: Images of the relative fraction of dissolved iron related recombination of total recombination for standard-growth mc-Si brick for injection levels ranging from 1x10^{11}-1x$10^{12}$$cm^{-3}$. No quantitative data could be extracted in the highly contaminated bottom and top sections of the bricks using the full-field measurement. These areas mostly appear in black. The bottom of the standard-growth brick was subsequently measured separately using a masking approach (see [9]) and is found to be nearly fully dominated by dissolved iron.

The second interesting measure that becomes accessible is the bulk lifetime due to other defects than dissolved iron. The respective data is shown in Figure 5 and reveals a considerable increase in bulk lifetime after removal of all interstitial iron for our sample. This is due to the dominant recombination through the as-grown interstitial iron contamination and already reasonable bulk lifetime values, indicating a relatively low contamination of other defects.

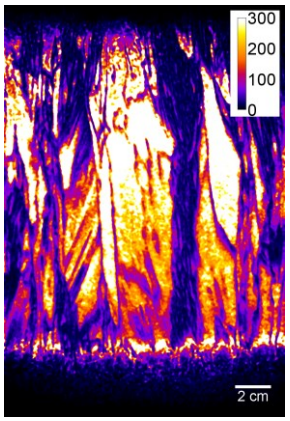

Figure 5: τ_{other}-image of standard growth Si brick depicting the as-grown bulk lifetime due to defects other than dissolved iron. The image is calculated from Figure 2 and Figure 3 using the SRH defect recombination model. Bulk lifetimes are given in µs for injection levels ranging from 1x10^{11}-1x$10^{12}$$cm^{-3}$. Due to the dominance of the interstitial iron defect, relatively high bulk lifetimes are reached after removal of iron indicating relatively low boron-oxygen or other defect concentrations.

4 DISCUSSION

All data shown is modelled one-dimensionally, a

simplification that breaks down in the vicinity of grain boundaries and dislocations clusters. The PL analysis convolutes information of varies depth of the top few millimeter. It has been found that only grains with at least 2 mm diameter can be analyzed quantitatively [14].

The accuracy of the technique is mostly defined by the uncertainty of the electron capture-cross-sections of Fe-B and Fe_i defect levels. These are somewhat difficult to estimate. Hence, more suitable methods to verify the accuracy are with measurement techniques that don't depend on the lifetime signature [15] or via simulations of the iron contamination in silicon ingots [16].

Figure 6 shows the comparison the measured cross-sectional average interstitial iron concentration with simulated data along the full ingot height. Details of the simulation are given in [9]. Good agreement is found for most parts of the ingot giving some confirmation of the measurement accuracy. The deviation in the very bottom indicate an increased measurement uncertainty in this region, which is largely caused by the low SNR and the more complex analysis procedure as outlined in [9]. The comparison gives confidence that especially the transition regions can be analyzed well with regard to position and concentration. Thus, a more sophisticated cutting guide may be based on this measurement.

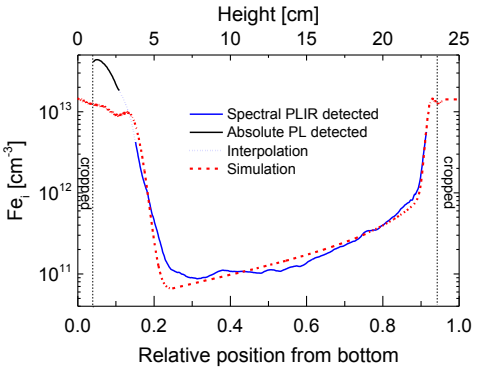

Figure 6: Measured and simulated iron concentration of a standard-growth mc-Si brick as a function of brick height. The simulated data is compared with a cross-sectional average concentration along a central large grain structure. The central data is measured using the spectral PLIR analysis, whereas the bottom section is analyzed through spectral PLIR calibrated absolute PL intensities discussed in [9]. The top and bottom section of the standard-growth brick were cropped prior to the measurement as indicated in the graph, hence could only be assessed experimentally in its remaining.

5 CONCLUSIONS

Quantitative spectral PL imaging has been demonstrated to also give access to the dissolved/interstitial iron concentration on silicon ingot/bricks. The measurement is confirmed independently by detailed simulations indicating good accuracy. True low injection conditions are a key feature for accuracy removing uncertainties arising from the estimation of any injection dependence or dissociation during measurement. The measurement can include the low-lifetime and highly contaminated bottom/top/edge region of the directionally solidified ingot, though currently with an increased complexity in procedure.

Measuring the dissolved iron concentration directly on silicon bricks can be done with simple sample preparation, which only involved a flash light based dissociation process. It is a non-contact method that is fully feasible to be extended to inline use. The measurement on silicon bricks offers access to unaltered as-grown contaminations that is otherwise only possible via health and risk sensitive HF passivation of many as-cut wafers.

Access to both bulk lifetime and interstitial iron concentration give rise to interesting measures of the relative recombination activity and may provide a measure to investigate other recombination defects and its impact. Interstitial iron is the dominant as-grown defect in the presented ingot. Knowledge of the bulk lifetime after complete or partial removal of dissolved iron may be useful for predictive measures.

The measurement information outlined may be used for appropriate pricing of wafer material.

REFERENCES

[1] B. Mitchell, T. Trupke, J.W. Weber, J. Nyhus, J. Appl. Phys. 109 (2011) 083111.

[2] B. Mitchell, J.W. Weber, D. Walter, D. Macdonald, T. Trupke, J. Appl. Phys. 112 (2012) 063116.

[3] B. Mitchell, M.K. Juhl, M.A. Green, T. Trupke, IEEE J. Photovoltaics 3 (2013) 962.

[4] A.A. Istratov, H. Hieslmair, E.R. Weber, Appl. Phys. A Mater. 69 (1999) 13.

[5] J. Schmidt, B. Lim, D. Walter, K. Bothe, S. Gatz, T. Dullweber, P.P. Altermatt, IEEE J. Photovoltaics 3 (2013) 114.

[6] D. Macdonald, J. Tan, T. Trupke, J. Appl. Phys. 103 (2008) 073710.

[7] A.Y. Liu, D. Macdonald, J. Appl. Phys. 115 (2014) 114901.

[8] F. Schindler, B. Michl, J. Schon, W. Kwapil, W. Warta, M.C. Schubert, IEEE J. Photovoltaics 4 (2014) 122.

[9] B. Mitchell, D. Macdonald, J. Schön, J.W. Weber, H. Wagner, IEEE J. Photovoltaics 4 (2014) 1185.

[10] G. Zoth, W. Bergholz, J. Appl. Phys. 67 (1990) 6764.

[11] B. Mitchell, J.W. Weber, M. Juhl, D. Macdonald, T. Trupke, Solid State Phenom. 205-206 (2013) 118.

[12] S.Y. Lim, D. Macdonald, Sol. Energy Mater. Sol. Cells 95 (2011) 2485.

[13] D.H. Macdonald, L.J. Geerligs, A. Azzizi, J. Appl. Phys. 95 (2004) 1021.

[14] B. Mitchell, J. Greulich, T. Trupke, Sol. Energy Mater. Sol. Cells 107 (2012) 75.

[15] S. Herlufsen, D. Macdonald, K. Bothe, J. Schmidt, Phys. Status Solidi - Rapid Res. Lett. 6 (2012) 1.

[16] M.C. Schubert, J. Schon, F. Schindler, W. Kwapil, A. Abdollahinia, B. Michl, S. Riepe, C. Schmid, M. Schumann, S. Meyer, W. Warta, IEEE J. Photovoltaics 3 (2013) 1250.